Sucrose Nonfermenting-Related Kinase Regulates Both Adipose Inflammation and Energy Homeostasis in Mice and Humans

Jie Li,[1,2,3] Bin Feng,[4,5] Yaohui Nie,[4] Ping Jiao,[4,6] Xiaochen Lin,[2,3] Mengna Huang,[2,3] Ran An,[2,7] Qin He,[4] Huilin Emily Zhou,[8] Arthur Salomon,[9,10] Kirsten S. Sigrist,[9] Zhidan Wu,[11] Simin Liu,[2,3,4] and Haiyan Xu[2,3,4,12]

Diabetes 2018;67:400–411 | https://doi.org/10.2337/db17-0745

OBESITY STUDIES

Sucrose nonfermenting-related kinase (SNRK) is a member of the AMPK-related kinase family, and its physiological role in adipose energy homeostasis and inflammation remains unknown. We previously reported that SNRK is ubiquitously and abundantly expressed in both white adipose tissue (WAT) and brown adipose tissue (BAT), but SNRK expression diminishes in adipose tissue in obesity. In this study we report novel experimental findings from both animal models and human genetics. SNRK is essential for survival; SNRK globally deficient pups die within 24 h after birth. Heterozygous mice are characterized by inflamed WAT and less BAT. Adipocyte-specific ablation of SNRK causes inflammation in WAT, ectopic lipid deposition in liver and muscle, and impaired adaptive thermogenesis in BAT. These metabolic disorders subsequently lead to decreased energy expenditure, higher body weight, and insulin resistance. We further confirm the significant association of common variants of the *SNRK* gene with obesity risk in humans. Through applying a phosphoproteomic approach, we identified eukaryotic elongation factor 1δ and histone deacetylase 1/2 as potential SNRK substrates. Taking these data together, we conclude that SNRK represses WAT inflammation and is essential to maintain BAT thermogenesis, making it a novel therapeutic target for treating obesity and associated metabolic disorders.

Obesity is characterized by massive expansion of white adipose tissue (WAT). Obesity-related inflammation is increasingly recognized as a causal factor in the development of insulin resistance and type 2 diabetes (1). Multiple types of immune cells have been identified in WAT of obese animals and humans (2–6), although the temporal order of infiltration by different types of immune cells is currently being investigated. Nevertheless, macrophages have been placed in the center of adipose inflammation because of their abundance in WAT and the large amount of proinflammatory cytokines they secrete, although adipocytes themselves are also a source of inflammatory factors (2,7,8). Inhibition of WAT macrophage infiltration can improve insulin sensitivity in obese mice (9) and is associated with body weight loss in obese humans (10,11). All existing antidiabetes remedies, including thiazolidinediones, dipeptidyl peptidase 4 inhibitors, metformin, incretin agonists, and even lifestyle

[1]National Key Discipline, Department of Nutrition and Food Hygiene, School of Public Health, Harbin Medical University, Harbin, China
[2]Department of Epidemiology, Brown University, Providence, RI
[3]Center for Global Cardiometabolic Health, Brown University, Providence, RI
[4]Hallett Center for Diabetes and Endocrinology, Rhode Island Hospital, Warren Alpert Medical School of Brown University, Providence, RI
[5]Animal Nutrition Institute, Sichuan Agricultural University, Chengdu, Sichuan Province, China
[6]School of Pharmaceutical Sciences, Jilin University, Changchun, Jilin Province, China
[7]Department of Pharmaceutical Analysis and Analytical Chemistry, College of Pharmacy, Harbin Medical University, Harbin, China
[8]Sharon High School, Sharon, MA
[9]Department of Molecular Biology, Cell Biology and Biochemistry, Brown University, Providence, RI
[10]Department of Chemistry, Brown University, Providence, RI
[11]Musculoskeletal Disease Area, Novartis Institutes for Biomedical Research, Cambridge, MA
[12]Merck & Co., Boston, MA

Corresponding authors: Haiyan Xu, haiyan_xu@brown.edu, and Simin Liu, simin_liu@brown.edu.

Received 29 June 2017 and accepted 15 December 2017.

This article contains Supplementary Data online at http://diabetes.diabetesjournals.org/lookup/suppl/doi:10.2337/db17-0745/-/DC1.

J.L. and B.F. contributed equally to this work.

interventions, essentially exhibit anti-inflammatory activity (1,12–14).

In contrast to WAT, brown adipose tissue (BAT) is a thermogenic organ whose mass is inversely correlated with BMI and age (15). BAT expresses uncoupling protein 1 (UCP1), which uncouples mitochondrial respiration from ATP synthesis. Two types of BAT exist: the classic interscapular-like brown adipocytes and inducible brown adipocytes interspersed among subcutaneous white fat depots in response to exposure to cold or elevated plasma concentrations of catecholamine (beige adipocytes) (15). In particular, the discovery of functional BAT in humans has revitalized interest in targeting this nonshivering thermogenic tissue to treat obesity and its related disorders (16).

We report herein a series of experimental studies investigating the regulatory roles of sucrose nonfermenting-related kinase (SNRK) in the development of both adipose tissue inflammation and adaptive thermogenesis. SNRK is a member of the AMPK/SNF1 family, and its functional roles have been underinvestigated. WAT and BAT predominantly express SNRK, and normal cell growth and function require it (17). SNRK is a completely different protein from sucrose nonfermenting AMPK-related kinase, whose expression is very low in adipose tissue (18–20). SNRK expression is decreased in WAT of obese mice, whereas knocking down SNRK in cultured white adipocytes increases inflammatory responses (17). SNRK has also been shown to play a role in neuronal cell apoptosis, inhibit proliferation of colon cancer cells, and contribute to the development of angioblasts in zebra fish and of cardiac metabolism in mice (21–27).

In this article, we report novel findings concerning the critical role of SNRK in adipose tissue inflammation and energy homeostasis. By characterizing both SNRK heterozygous and adipocyte-specific SNRK knockout mice, we found that the absence of SNRK is sufficient to cause adipose tissue inflammation and impair adaptive thermogenesis. Furthermore, we identified common variants in the *SNRK* gene that directly associate with obesity in a large, well-characterized national cohort of women in the U.S.

RESEARCH DESIGN AND METHODS

Reagents and Cells

Primary brown adipocytes were isolated and transformed with SV40 large T antigen, as previously described (28). 3T3-L1 coxsackievirus and adenovirus receptor–expressing (CAR) cells were provided by Orlicky et al. (29) (University of Colorado Health Sciences Center). Preadipocytes were differentiated as previously described (30). Dexamethasone, insulin, isobutylmethylxanthine, and CL316,243 were purchased from Sigma. c-Jun N-terminal kinase (JNK) antibody was purchased from Santa Cruz Biotechnology. Phospho-JNK antibody was purchased from Cell Signaling Technology. SNRK antibody was purchased from the University of Dundee (31). UCP1 antibody was purchased from Millipore. F4/80 antibody was purchased from Serotec. Tubulin antibody was purchased from Abcam. A histone deacetylase (HDAC) 1 activity kit was purchased from BPS Bioscience.

Generation of Global and Adipose-Specific SNRK-Deficient Mice

The targeting vector was purchased from KOMP. Electroporation of embryonic stem (ES) cells in C57BL/6J background was performed at the transgenic facility at Brown University. To generate adipose-specific SNRK knockout mice, the LacZ/Neo cassette was removed from the germ line by breeding $SNRK^{+/-}$ mice with ROSA26FlpO transgenic mice on a C57BL/6 background; SNRK alleles were restored to those of the wild type (WT), except exon 4 was left to be flanked by Lox P sites. After breeding the FlpO recombinase transgene out of the system, $SNRK^{loxp+/+}$ mice were mated with adiponectin-Cre (A-Cre) transgenic mice, followed by intercrossing, to generate $SNRK^{fat-/-,\ A\text{-}cre}$ mice. $SNRK^{loxp/loxp}$ and $SNRK^{A\text{-}cre}$ littermates were used as controls.

Mice Maintenance and Analysis

Mice were fed either a normal chow diet or a high-fat diet (HFD; 60% kcal from fat; D12492; Research Diets, Inc.) starting at 4 weeks of age for 20 weeks. Body weight and blood glucose levels in a fed state were measured weekly and biweekly, respectively. At the end of the study, tissues were rapidly dissected and frozen or fixed for further studies. To study thermogenesis, CL316,243 (1 mg/kg) was injected for seven consecutive days. All animal procedures used in our studies were approved by the Institutional Animal Care and Use Committees of Rhode Island Hospital and Brown University.

Indirect Calorimetry

Oxygen consumption (VO_2), carbon dioxide production (VCO_2), and food intake were measured individually over 24 h using a Comprehensive Lab Animal Monitoring System (Columbus Instruments) after 1 day of acclimation. During the experiment, mice had free access to food and water. Energy expenditure was calculated using the formula $VO_2 \times (3.815 + 1.232 \times \text{Respiratory quotient})$, and normalized to $(\text{body mass})^{0.75}$ (25).

SNRK Activity Assay

SNRK was immunoprecipitated from adipose tissue and washed four times with wash buffer, followed by four more washes with buffer A. Kinase was assayed at 30°C for 30 min in a shaking water bath. The reaction occurred in 40 μL buffer A (total volume) containing 10 μci γ-^{32}P-ATP, 200 μmol/L AMARA peptide, 1 mmol/L ATP, and 10 mmol/L magnesium acetate. The reaction was terminated by adding 2.1 cm of P81 phosphocellulose paper to the mixture. The P81 paper was put into a scintillation vial and washed four times with 0.5% phosphoric acid then once with water before counting.

Glucose and Insulin Tolerance Tests

For the glucose tolerance test, mice were fasted overnight and then injected with glucose at a dose of 1 g/kg for chow-fed

male mice, 1.5 g/kg for chow-fed female mice, 0.5 g/kg for HFD-fed male mice, and 0.75 g/kg for HFD-fed female mice. For the insulin tolerance test, mice were fasted for 6 h and injected with insulin at a dose of 0.75 U/kg for chow-fed male mice and 0.5 U/kg for chow-fed female mice and HFD-fed mice.

RNA Extraction and Real-time PCR Analysis

RNA samples were extracted from tissues or isolated cells using the TRIzol reagent or the RNAeasy kit, according to the manufacturer's instructions. DNase I–treated RNA samples were reverse-transcribed to generate cDNA. Real-time PCR analysis was performed using Power SYBR Green RT-PCR Reagent on an ABI prism thermal cycler (StepOnePlus; Applied Biosystems). *28S* rRNA was used as a reference gene for normalization in each reaction.

Western Blotting Analysis

Proteins were separated on 4–12% Bis-Tris-PAGE gel, transferred onto polyvinylidene difluoride membranes, then incubated for 1 h with 1× Tris-buffered saline supplemented with 5% nonfat dry milk. Membranes then were incubated with the corresponding primary antibodies at 4°C overnight. After thorough washes in 1× Tris-buffered saline with Tween, membranes were incubated with corresponding horseradish peroxidase–linked secondary antibodies at room temperature for 1 h. Signals were detected with a chemiluminescence Western blotting detection solution (PerkinElmer) on the Alpha Innotech FluorChem imaging system.

Histological Analysis

Tissues were fixed in 10% neutrally buffered formalin for 1 day, then transferred to 70% ethanol and embedded in paraffin. Hematoxylin-eosin staining, immunohistochemistry of UCP1 and F4/80, as well as Oil Red O staining were done at the core laboratory of Rhode Island Hospital.

Statistical Analysis

Results of mouse studies are presented as the mean ± SEM. Statistical significance was determined at $P < 0.05$. The two-tailed Student *t* test was used to compare differences between groups, and ANOVA was used to compare among three groups.

RESULTS

Regulation of SNRK Activity in White Adipocyte and Adipose Tissue

To understand the role SNRK plays in WAT energy homeostasis, we assessed changes in SNRK activity in response to nutrition status. SNRK activity was significantly decreased in WAT of lean mice upon overnight fasting compared with that in mice fed the chow diet (Fig. 1*A*). Moreover, SNRK activity also significantly reduced in cultured white adipocytes when serum was removed (the nonselective β-adrenergic receptor agonist isoproterenol seems to activate SNRK only in the presence of serum; Fig. 1*B* and *C*). The β3 adrenergic receptor agonist CL316,243 activated SNRK in subcutaneous adipose tissue (Fig. 1*D*). These experimental data indicate that SNRK promotes energy use in response to nutrient influx.

Interestingly, chow diet feeding activated SNRK, whereas chronic HFD feeding diminished SNRK activity (Fig. 1*E*). Chow diets are typically high in carbohydrates and deliver energy to adipocytes in the form of glucose; the HFD supplies energy in the form of free fatty acids (FFA). Experimental data indicate that SNRK expression can be increased by glucose but decreased by FFA (Supplementary Fig. 1), consistent with our observation that the carbohydrate-rich chow diet increases, whereas the fat-rich diet diminishes, SNRK activity.

Regulation of SNRK Expression in BAT

SNRK expression was decreased significantly in the classic BAT of ob/ob and DIO mice compared with that in lean controls (Fig. 2*A* and *C*). This decrease of SNRK activity was consistent with gene expression (Fig. 2*B*). Expression of SNRK in BAT of ob/ob mice was significantly increased by leptin (Fig. 2*D*). Upon exposure to cold (4°C), SNRK mRNA levels in BAT were quickly and significantly upregulated in 3 h (Fig. 2*E*). The elevation of *SNRK* gene expression remained significantly higher than that in control mice housed at room temperature (22°C) for up to 6 h. The pattern of *SNRK* gene expression regulation by exposure to cold was similar to those of UCP1 and peroxisome proliferator–activated receptor γ coactivator 1α (PGC-1α) (data not shown). SNRK expression in WAT was also upregulated

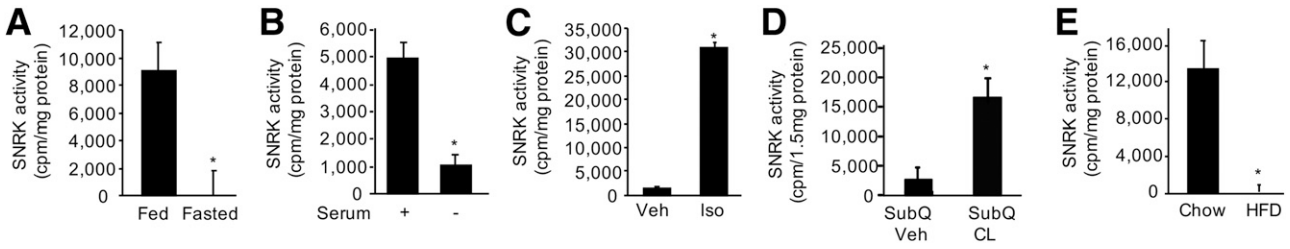

Figure 1—SNRK activity in WAT and cultured adipocytes. *A*: SNRK activity in WAT of chow-fed vs. fasted lean mice (n = 3 mice/group). *B*: SNRK activity in cultured white adipocytes in the presence (+) or absence (−) of serum for 18 h. *C*: SNRK activity in cultured white adipocytes treated with 10 μmol/L isoproterenol (Iso) or vehicle (Veh) in the presence of serum for 1 h. *D*: SNRK activity in subcutaneous adipose tissue (SubQ) of chow-fed lean mice treated with 100 nmol/L CL316,243 (CL) or vehicle (Veh) for 4 h (n = 3 or 4 mice/group). *E*: SNRK activity in gonadal WAT of mice fed the chow diet vs. the HFD for 20 weeks (n = 5 mice/group). *$P < 0.05$.

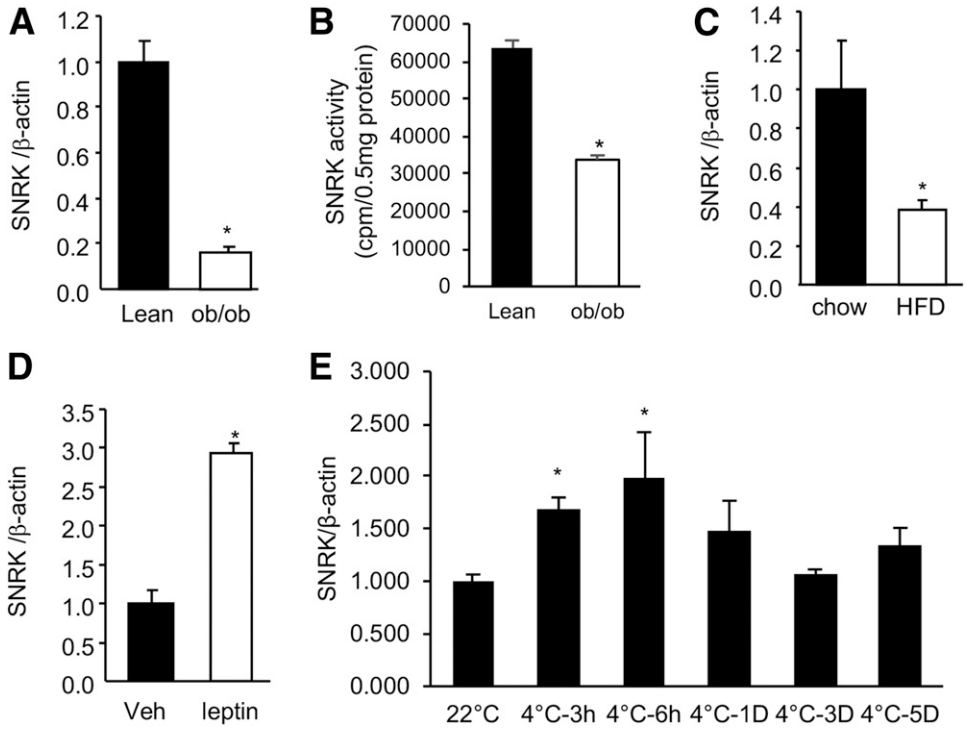

Figure 2—Regulation of *SNRK* gene expression in BAT. *A*: *SNRK* gene expression in BAT of lean vs. ob/ob mice (n = 3 mice/group). *B*: SNRK activity in BAT of lean vs. ob/ob mice (n = 4 mice/group). *C*: *SNRK* gene expression in BAT of mice fed the chow diet vs. the HFD for 20 weeks (n = 5 mice/group). *D*: *SNRK* gene expression in BAT of ob/ob mice treated with vehicle (Veh) or leptin at 10 mg/kg for 24 h (n = 3 mice/group). *E*: *SNRK* gene expression in BAT of lean mice (n = 4 mice/group) at room temperature vs. 4°C for 3 h, 6 h, 1 day (1D), 3 days (3D), and 5 days (5D). *$P < 0.05$ compared with controls.

by exposure to cold, indicating that SNRK may play a critical role in adaptive thermogenesis (data not shown).

Heterozygous SNRK Mice Are Leaner But Have Inflamed WAT and Less BAT

To understand the physiological role of SNRK in adipose metabolism, we first generated global SNRK knockout mice. The SNRK targeting vector was constructed with tissue-specific knockout potential, as shown in Supplementary Fig. 2. A LacZ/neo cassette was designed to insert between exons 3 and 4, disrupting splicing of endogenous SNRK exons and therefore creating a knockout phenotype. To improve the time efficiency from backcrossing, we used embryonic stem ES cells on a C57BL/6J background for electroporation.

Global deficiency of SNRK is lethal; SNRK knockout pups die on the second day after birth. This phenotype of perinatal lethality may be due to cardiac dysfunction in the absence of SNRK (25). β-Galactosidase staining in $SNRK^{-/-}$ pups showed ubiquitous LacZ activity (Supplementary Fig. 3*A*). We found no differences in body weight among WT, $SNRK^{+/-}$, and $SNRK^{-/-}$ pups at birth (Supplementary Fig. 3*B*). Further examination several hours after birth revealed that blood glucose levels of $SNRK^{-/-}$ pups were significantly lower than those of WT pups (Supplementary Fig. 3*C*).

We therefore characterized SNRK heterozygous mice fed either the chow diet or the HFD. On a chow diet, male $SNRK^{+/-}$ mice were indistinguishable from WT mice at 4 weeks of age, but they became significantly leaner by 22 weeks of age (Supplementary Fig. 4*A*). The mass of epididymal and subcutaneous WAT decreased significantly in $SNRK^{+/-}$ mice—by 40% and 50%, respectively (Supplementary Fig. 4*B*). Triacylglyceride (TAG) contents of these two WAT depots also decreased significantly—by 33% and 43%, respectively (Supplementary Fig. 4*C*). Gene expression analysis indicated that SNRK heterozygosity inflamed WAT, as reflected by significantly increased expression of tumor necrosis factor (TNF)-α and CD11c (Supplementary Fig. 4*D*). By contrast, expression of adipogenic transcription factors (peroxisome proliferator–activated receptor γ and C/EBPα) and insulin-sensitizing adipokines (leptin and adiponectin) decreased significantly in WAT of $SNRK^{+/-}$ mice compared with that of WT mice (Supplementary Fig. 4*D*). Histology study further revealed the existence of a crownlike structure in WAT of $SNRK^{+/-}$ mice (Supplementary Fig. 4*E*). These experiments indicated that SNRK haploinsufficiency likely caused $CD11c^{+}$ macrophages to accumulate in WAT. We observed no differences in body weight or fat pad weight between WT and $SNRK^{+/-}$ mice consuming the HFD, but $SNRK^{+/-}$ mice eating the HFD had significantly higher fasting blood glucose levels than WT mice (Supplementary Fig. 5*A*–*C*).

SNRK heterozygosity significantly decreased BAT mass by about 33% (Supplementary Fig. 6*A*). Histological studies also indicated smaller brown adipocytes and less lipid accumulation in BAT of these $SNRK^{+/-}$ mice (Supplementary

Fig. 6*B* and *C*). BAT depots from SNRK$^{-/-}$ pups had significantly reduced PRDM16 and UCP1 mRNA levels (by ~60%) compared with WT mice (Fig. 3*A*). Immunoblot analysis and immunohistochemistry also confirmed decreased UCP1 protein expression in BAT of SNRK$^{-/-}$ pups (Fig. 3*B* and *C*). Oil Red O staining revealed the absence of lipid droplets in BAT of SNRK$^{-/-}$ pups (Fig. 3*D*). Electron microscopy also demonstrated lower mitochondrial density and occasional ruptures of mitochondrial cristae (Fig. 3*E*, arrows).

Adipose-Specific SNRK Deficiency Inflames Adipose Tissue and Impairs Thermogenesis

To understand the role of adipocyte SNRK in whole-body energy homeostasis, we next created adipose tissue–specific SNRK knockout mice using adiponectin promoter–driven Cre recombinase expression (SNRK$^{fat-/-,\ A\text{-}Cre}$). Real-time PCR confirmed efficient SNRK deletion in WAT (Fig. 4*A*) and BAT (Fig. 5*A*). SNRK$^{fat-/-,\ A\text{-}Cre}$ mice appeared to have smaller adipocytes than littermate controls and show macrophage accumulation in WAT, as indicated by immunostaining using F4/80 antibody, a commonly used macrophage marker (Fig. 4*B*, bottom panels, brown). Real-time PCR analysis revealed significantly increased expression of TNF, interleukin-6, and monocyte chemoattractant proteins (MCP) 1, 2, and 3 in adipocytes isolated from SNRK$^{fat-/-,\ A\text{-}Cre}$ mice compared with littermate control mice (Fig. 4*C*). Expression levels of F4/80 and CD11c were also significantly increased but *ATG12* gene expression was significantly decreased (Fig. 4*D*). Plasma levels of cytokines and chemokines also significantly increased (Fig. 4*E*) in these SNRK$^{fat-/-,\ A\text{-}Cre}$ mice, which were also glucose intolerant and insulin resistant (Fig. 4*F* and *G*).

Unlike SNRK$^{+/-}$ mice, however, SNRK$^{fat-/-,\ A\text{-}Cre}$ mice appeared significantly heavier than littermate SNRK$^{loxp/loxp}$ and SNRK$^{A\text{-}Cre}$ control mice (Fig. 5*B*), suggesting that the body weight reduction observed in SNRK$^{+/-}$ mice was most likely a secondary effect due to reduced SNRK expression in nonadipose tissues. To understand the mechanism of increased body weight, we performed a metabolic cage study and found that SNRK$^{fat-/-,\ A\text{-}Cre}$ mice have decreased energy expenditure (Fig. 5*C*) and UCP1 protein expression in BAT (Fig. 5*F*). In addition, F4/80 immunohistochemistry indicated a large number of macrophages in BAT of SNRK$^{fat-/-,\ A\text{-}Cre}$ mice (Fig. 5*F*), which was confirmed by significantly increased *F4/80* and *CD11c* gene expression

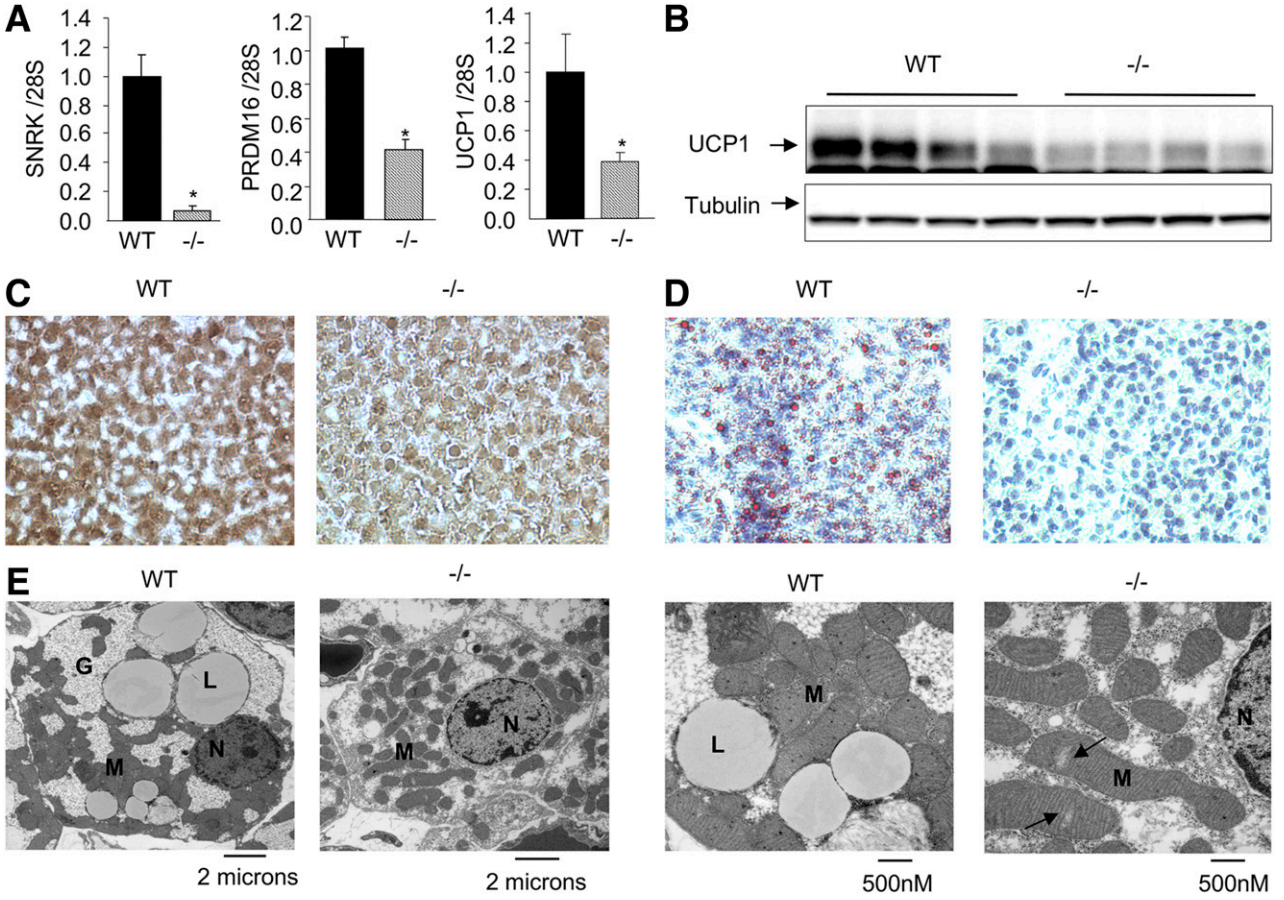

Figure 3—BAT from SNRK$^{-/-}$ and littermate WT control newborn pups. *A* and *B*: Gene expression (n = 7–9 pups/group) (*A*) and UCP1 protein expression (n = 4 pups/group) (*B*) in BAT of SNRK$^{-/-}$ and littermate WT newborn pups. *$P < 0.05$. *C–E*: UCP1 immunostaining (*C*), Oil Red O staining (*D*), and electron microscopy (*E*) of BAT from SNRK$^{-/-}$ and littermate WT newborn pups. Arrows indicate lower mitochondrial density and occasional ruptures of mitochondrial cristae. G, glycogen; L, lipid droplet; M, mitochondria; N, nucleus.

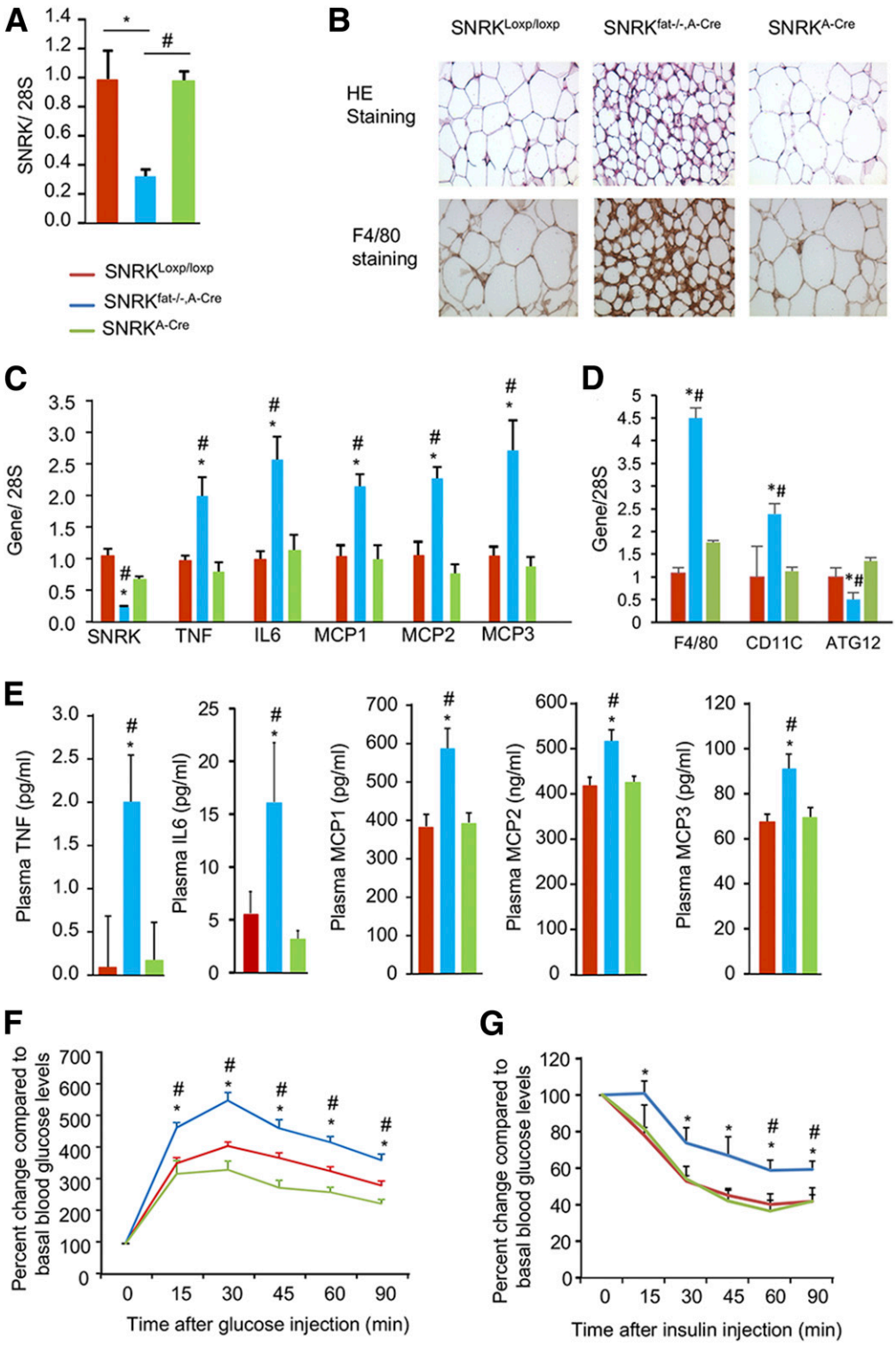

Figure 4—Characterization of adipose tissue–specific SNRK knockout ($SNRK^{fat-/-,\ A\text{-}Cre}$) and littermate control ($SNRK^{loxp/loxp}$, $SNRK^{A\text{-}Cre}$) mice. *A*: *SNRK* gene expression in WAT of $SNRK^{loxp/loxp}$, $SNRK^{fat-/-,\ A\text{-}Cre}$, and $SNRK^{A\text{-}Cre}$ mice (n = 3 or 4 mice/per group). *B*: Histology of the subcutaneous WAT depot stained with hematoxylin-eosin (HE; upper panels) or F4/80 antibody (lower panels). *C*: Expression of cytokine and chemokine genes in primary adipocytes isolated from $SNRK^{fat-/-,\ A\text{-}Cre}$ and littermate control mice (n = 7–12 mice/group). *D*: Expression of *F4/80*, *CD11c*, and *ATG12* genes in gonadal WAT from $SNRK^{fat-/-,\ A\text{-}Cre}$ and littermate control mice (n = 4 mice/group). *E*: Plasma cytokine and chemokine levels in $SNRK^{fat-/-,\ A\text{-}Cre}$ and littermate control mice (n = 7–12 mice/group). *F*: Glucose tolerance test results from $SNRK^{fat-/-,\ A\text{-}Cre}$ mice and littermate control mice fed a chow diet (n = 7–12 mice/group). *G*: Insulin tolerance test results from $SNRK^{fat-/-,\ A\text{-}Cre}$ mice (n = 8 mice/group) and littermate control mice fed (n = 5–9 mice/group) fed an HFD for 20 weeks. *$P < 0.05$, $SNRK^{fat-/-,\ A\text{-}Cre}$ vs. $SNRK^{loxp/loxp}$; #$P < 0.05$, $SNRK^{fat-/-,\ A\text{-}Cre}$ vs. $SNRK^{A\text{-}Cre}$. IL, interleukin.

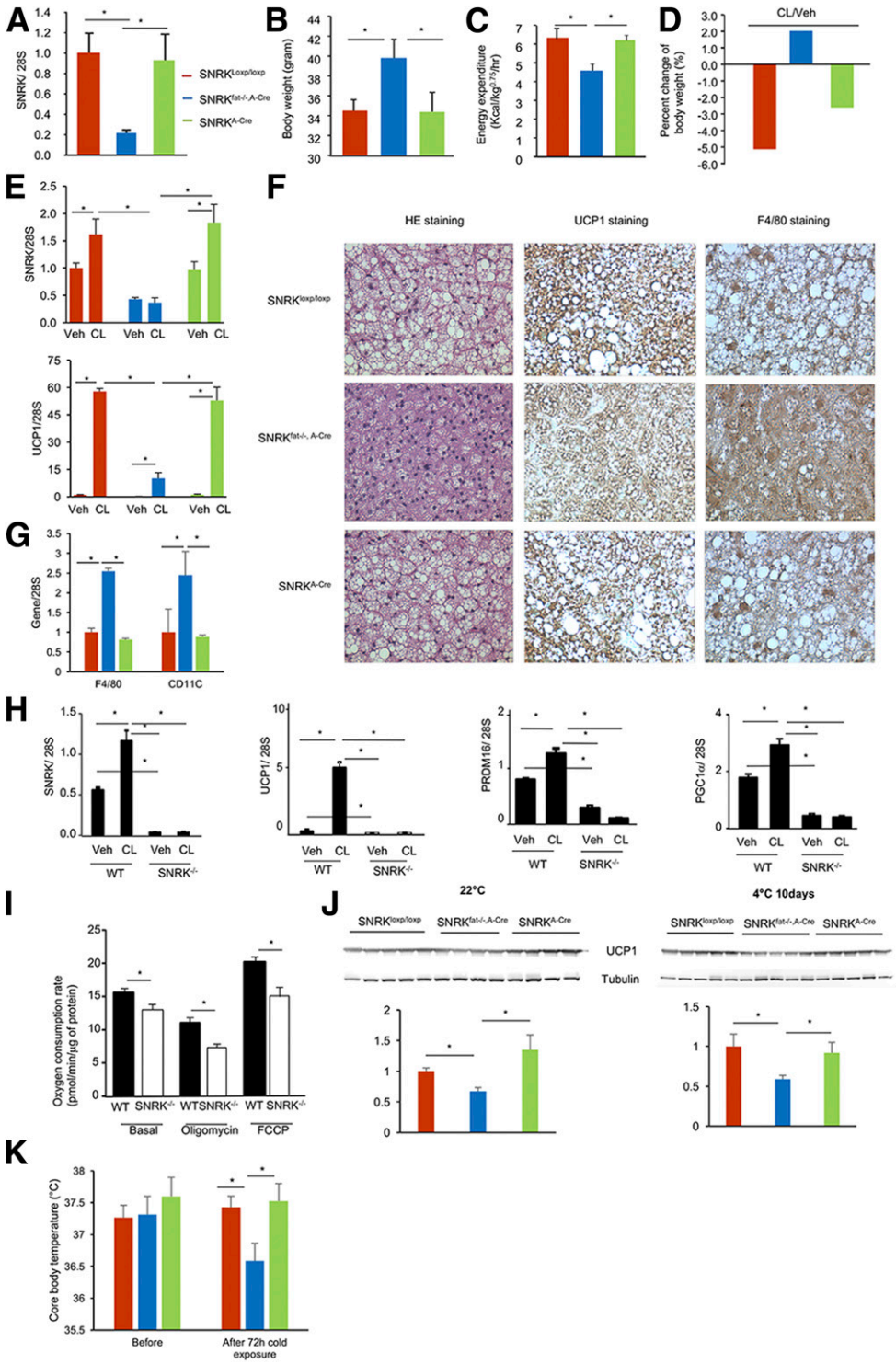

Figure 5—Effect of adipose SNRK deficiency on body weight and energy expenditure. *A*: *SNRK* gene expression in BAT of SNRK$^{loxp/loxp}$, SNRK$^{fat-/-,\ A\text{-}Cre}$, and SNRK$^{A\text{-}Cre}$ mice (n = 3 or 4 mice/group). *B* and *C*: Body weight (n = 6–12 mice/group) (*B*) and energy expenditure (n = 4 mice/group) (*C*) of SNRK$^{fat-/-,\ A\text{-}cre}$ and littermate control mice. *D*: Percentage change in body weight of SNRK$^{fat-/-,\ A\text{-}cre}$ and littermate control mice treated with CL316,243 (CL) or vehicle (Veh) (n = 3 or 4 mice/group). *E*: *SNRK* and *UCP1* gene expression in subcutaneous adipose tissue of SNRK$^{fat-/-,\ A\text{-}cre}$ and littermate control mice treated with Veh or CL (n = 3 or 4 mice/group). *F*: Hematoxylin-eosin (HE), UCP1, and F4/80 staining of BAT from SNRK$^{fat-/-,\ A\text{-}cre}$ and littermate control mice. *G*: Expression of *F4/80 and CD11c* genes in BAT from SNRK$^{fat-/-,\ A\text{-}Cre}$ and littermate control mice (n = 4 mice/group). *H*: Expression of *SNRK* and thermogenic genes in primary brown adipocytes differentiated from brown preadipocytes isolated from Veh- or CL-treated SNRK$^{-/-}$ and littermate WT newborn pups. *I*: Oxygen consumption by primary brown adipocytes as described in *H* under basal or treated conditions. *J*: UCP1 protein levels in BAT from SNRK$^{fat-/-,\ A\text{-}Cre}$ and littermate control mice (n = 4 or 5 mice/group) at 4°C and 22°C. *K*: Change in core body temperature of SNRK$^{fat-/-,\ A\text{-}Cre}$ and littermate control mice (n = 4–8 mice/group) upon exposure to cold for 72 h. *$P < 0.05$.

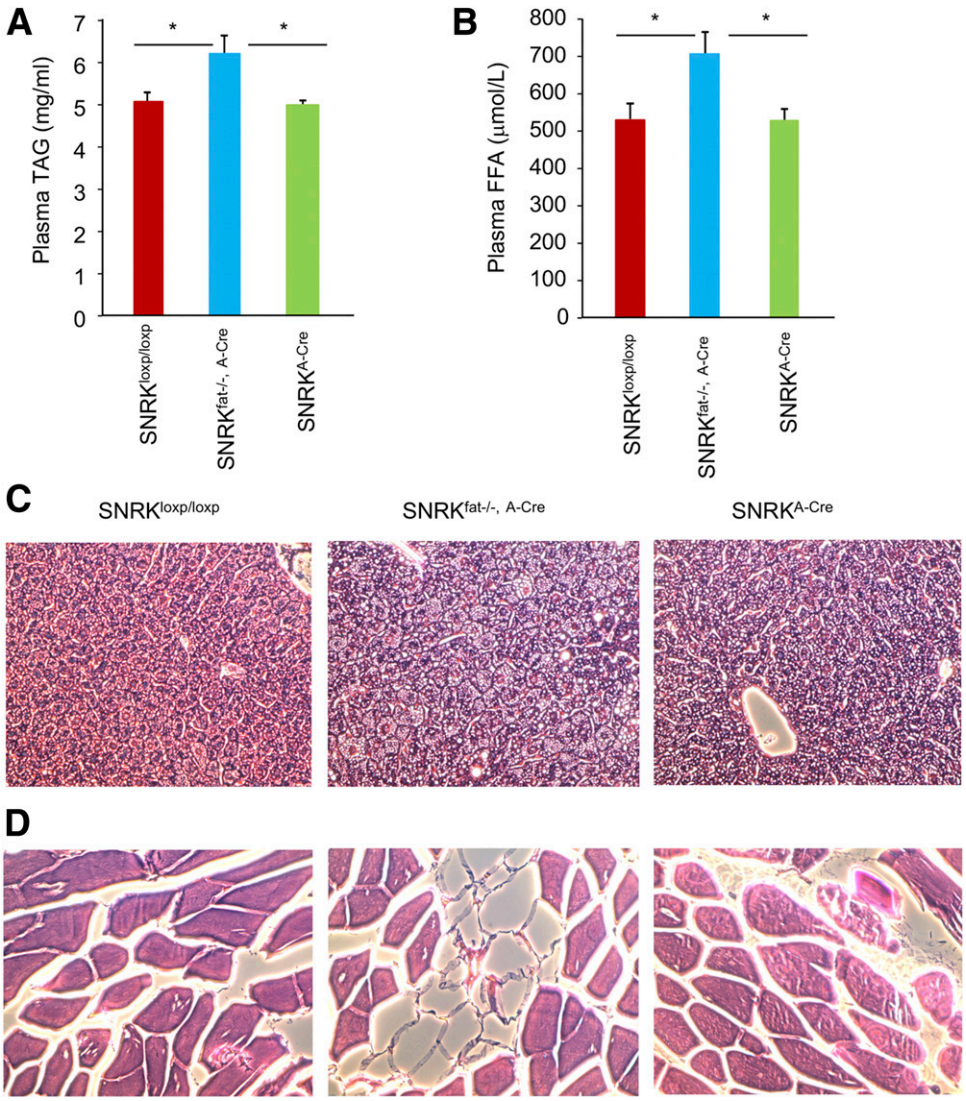

Figure 6—Lipid profile of adipose tissue–specific SNRK knockout mice. *A* and *B*: Plasma TAG (*A*) and FFA (*B*) levels in SNRK$^{fat-/-,\ A\text{-}Cre}$ and littermate control mice (n = 7–12 mice/group). *$P < 0.05$. *C* and *D*: Hematoxylin-eosin staining of livers (*C*) and muscles (*D*) from SNRK$^{fat-/-,\ A\text{-}Cre}$ and littermate control mice.

(Fig. 5*G*). To investigate whether decreased energy expenditure was due to impaired thermogenesis, we treated SNRK$^{fat-/-,\ A\text{-}Cre}$ and control mice with CL316,243, a highly selective β3 adrenergic receptor agonist that has an antiobesity effect by promoting thermogenesis and WAT browning. We found that SNRK$^{fat-/-,\ A\text{-}Cre}$ mice were fully resistant to CL316,243 (CL)-induced body weight reduction (Fig. 5*D*). Real-time PCR analysis confirmed that CL markedly induced SNRK and UCP1 expression in subcutaneous WAT of littermate control mice, but these effects were significantly blunted by SNRK deficiency in adipocytes (Fig. 5*E*). Primary brown adipocytes isolated from BAT of SNRK$^{fat-/-,\ A\text{-}Cre}$ mice also had a significantly blunted response to CL-induced SNRK, UCP1, PRDM16, and PGC-1α expression (Fig. 5*H*). In addition, primary brown adipocytes had significantly reduced basal and uncoupled respiration (Fig. 5*I*). UCP1 protein expression level was significantly decreased in BAT of SNRK$^{fat-/-,\ A\text{-}Cre}$ mice (Fig. 5*J*) and core body temperature was significantly lower in SNRK$^{fat-/-,\ A\text{-}Cre}$ mice after 72 h of exposure to cold (Fig. 5*K*).

Adipose mass of SNRK$^{fat-/-,\ A\text{-}Cre}$ mice was not significantly bigger than that of control mice, and increased body weight was most likely due to ectopic energy storage in other tissues. Indeed, we found that plasma FFA and TAG levels were significantly elevated in SNRK$^{fat-/-,\ A\text{-}Cre}$ mice compared with littermate controls (Fig. 6*A* and *B*). Livers of chow-fed SNRK$^{fat-/-,\ A\text{-}Cre}$ mice showed increased lipid accumulation, and adipocytes had infiltrated between muscle fibers in muscles of SNRK$^{fat-/-,\ A\text{-}Cre}$ mice (Fig. 6*C* and *D*).

Understanding the SNRK Signaling Pathway

To illustrate all possible SNRK targets, we performed a phosphoproteomic study by overexpressing SNRK in

hepatocytes and knocking down SNRK in cultured 3T3-L1 CAR adipocytes (17) (Supplementary Table 1). By searching for overlapping proteins with a phosphorylation pattern regulated in the opposite direction, we identified two candidates: eukaryotic elongation factor 1δ (EEF1D) and HDAC1, both of which regulate translation and transcription. In the SNRK knockdown experiment, phosphorylation of EEF1D on S133 decreased by 62% and phosphorylation of HDAC1 on S393 decreased by 82%. In the SNRK overexpression experiment, phosphorylation of EEF1D on S133 increased 2.5-fold and phosphorylation of HDAC1 on S393 increased 1.7-fold. To test further the functional relevance of EEF1D and HDAC1 in adipocyte inflammation, we knocked down EEF1D in 3T3-L1 CAR adipocytes and found that expression of proinflammatory cytokines and monocyte chemotactic factors increased significantly (Fig. 7*A* and *B*). In contrast to EEF1D, HDAC1 knockdown in 3T3-L1 CAR adipocytes did not recapitulate the phenotype caused by SNRK knockdown (data not shown). HDAC1 and HDAC2 proteins are functionally redundant in many tissues (32–35). S394 of HDAC2 is the equivalent of S393 of HDAC1 (36). However, simultaneous depletion of both HDAC1 and HDAC2 in 3T3-L1 CAR adipocytes significantly increased the expression of proinflammatory cytokines, monocyte chemotactic factors, and apoptotic chop; induced lipolysis; and activated JNK (Fig. 7*C–F*). Both EEF1D and HDAC1 can be coimmunoprecipitated with SNRK (Fig. 7*G*), and HDAC1 activity in gonadal WAT was found to be significantly lower in $SNRK^{fat-/-,\ A\text{-}Cre}$ mice (Fig. 7*H*).

Common SNRK Variants Link to Obesity in a Human Population

Finally, we searched for comparable human genetics evidence to support a role of SNRK in energy homeostasis by analyzing genome-wide association data from the Women's Health Initiative. Baseline characteristics of these women are shown in Supplementary Table 2. After adjusting for age, region, and global ancestry, two single nucleotide polymorphisms (rs4682880 and rs4682676) located in the upstream intergenic region of the *SNRK* gene were identified to be associated with BMI, waist circumference, and risk of obesity (Supplementary Fig. 7 and Supplementary Table 3).

DISCUSSION

In this study we investigated the role of SNRK in adipose tissue inflammation and energy homeostasis using an adipocyte-specific knockout mouse model. We previously identified SNRK as a suppressor of adipocyte inflammation in cultured 3T3-L1 CAR adipocytes by knocking down SNRK (17). This finding was confirmed using adipose-specific SNRK knockout mice. In this study, WAT SNRK seems to sense an influx of energy and suppress overnutrition-induced adipose tissue inflammation. This notion is supported by the observation of increased WAT SNRK activity upon feeding and treatment with a β adrenergic receptor agonist. By contrast, the absence of SNRK increases expression of inflammatory factors in WAT and elevates circulating levels of inflammatory cytokines. Loss of SNRK specifically in adipocytes increases body weight but does not significantly change the size of the WAT depot. Increased TAG and FFA levels in circulation, increased TAG in liver, and the presence of WAT in muscle indicate that the increased body weight may be due to ectopic lipid deposition in other tissues.

We previously observed that SNRK knockdown in cultured 3T3-L1 CAR adipocytes significantly decreased phosphorylation of multiple components in the mammalian target of rapamycin complex 1 signaling pathway (17). However, inhibition of mammalian target of rapamycin by rapamycin only recapitulated a small fraction of the phenotypes caused by SNRK knockdown, suggesting the existence of other substrates. In this study, through two reciprocal global phosphoproteomic (stable isotope labeling with amino acids in cell culture) studies of SNRK overexpression and knockdown, we revealed EEF1D and HDAC1/2 as potential SNRK downstream effectors, as reduced expression of these molecules in cultured white adipocytes recapitulate the majority of phenotypes manifested by SNRK knockdown. Both proteins can be coimmunoprecipitated with SNRK, and HDAC1 activity has been found to decrease significantly in WAT of $SNRK^{fat-/-,\ A\text{-}Cre}$ mice. EEF1D encodes subunit δ of the elongation factor 1 complex. S133 is reported to be the site responsible for EEF1D hyperphosphorylation induced by viral protein kinase, which is associated with increased elongation activity (37). Insulin can enhance the activity of the elongation factor 1 complex (38). HDAC function as transcription repressors by deacetylating lysine residues on histone proteins (39). Other genetic studies of animal models support the anti-inflammatory activities of HDAC1 and HDAC2 (40,41). Mice deficient in both HDAC1 and 2 specifically in intestinal epithelial cells have increased chronic inflammation on site (41).

In addition to suppressing adipose inflammation, SNRK is essential in regulating energy homeostasis in BAT, which we show here, to our knowledge for the first time. To date, the role of SNRK in energy homeostasis has been reported only for the heart. SNRK is essential for maintaining the function of the heart; lethality has been observed in cardiomyocyte-specific SNRK knockout mice between 8 and 10 months of age, including those with heterozygous loss of SNRK in cardiomyocytes (25,27). However, findings are inconsistent concerning the effect of SNRK on lipid metabolism in the heart (25,26). Cossette and colleagues (25,27) reported decreased fatty acid oxidation when SNRK expression was reduced in cardiomyocytes, with reductions of phospho-acetyl-CoA-carboxylase, phospho-AMPK, and Rho-associated kinase, whereas Rines et al. (26) reported increased fatty acid oxidation in hearts of SNRK knockout mice and decreased fatty acid oxidation with SNRK overexpression. Despite a protective effect of SNRK against ischemia/reperfusion, SNRK functions seem complex and may involve changes in mitochondria efficiency through decreasing UCP3 expression.

Our data demonstrate that global heterozygous loss of SNRK resulted in a decrease in body weight when mice were

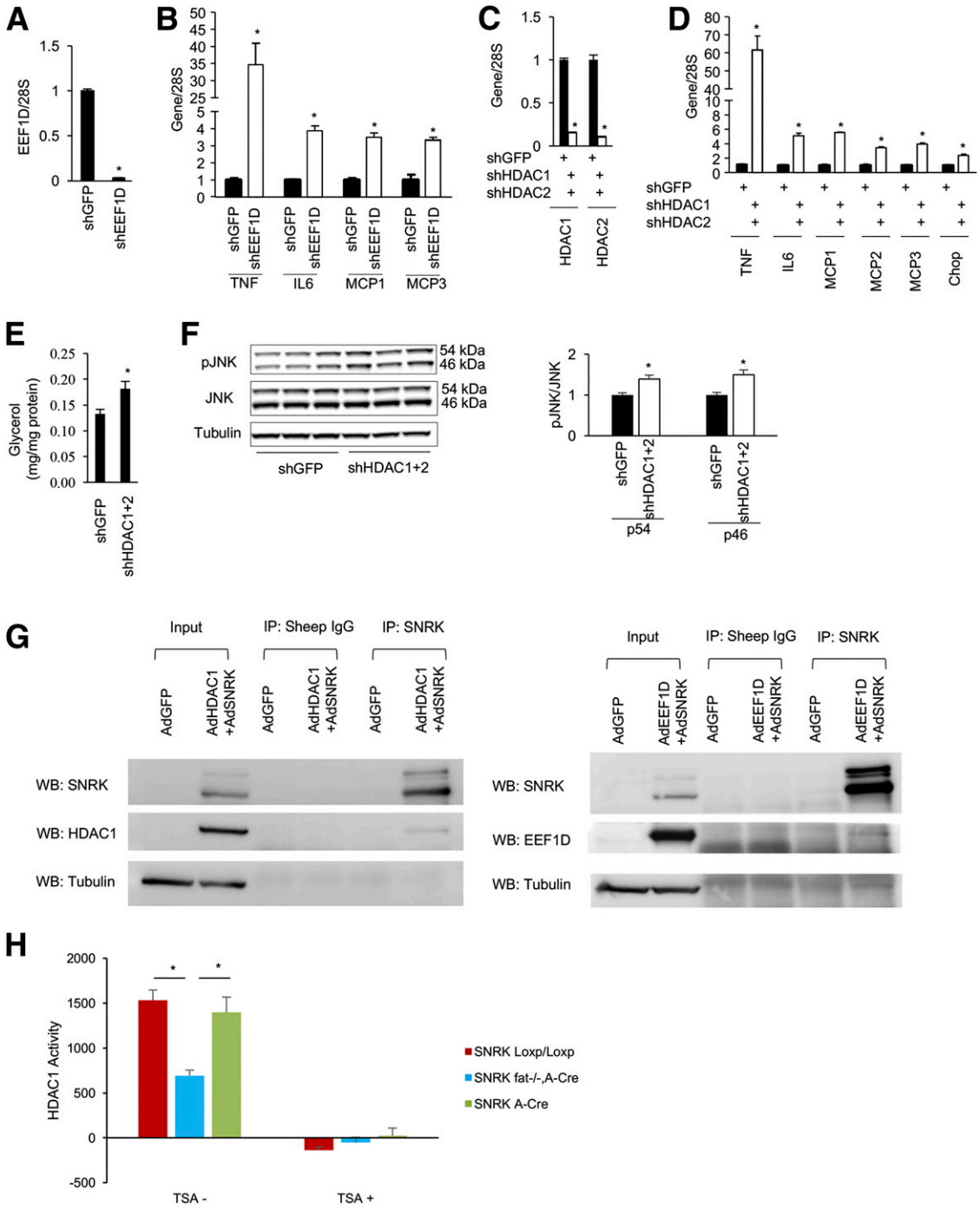

Figure 7—Reduction of EEF1D and HDAC1/2 expression in 3T3-L1 CAR adipocytes induces inflammation. Adenoviruses expressing interfering short hairpin (sh) RNA for green fluorescent protein (shGFP), EEF1D (shEEF1D), or HDAC1/2 (shHDAC1/2) were used to infect 3T3-L1 CAR adipocytes. *A*: shEEF1D effectively reduced EEF1D mRNA in 3T3-L1 CAR adipocytes. *B*: Effect of EEF1D knockdown on expression of *TNF*, *IL6*, *MCP1*, and *MCP3* genes. *C*: shHDAC1/2 effectively reduced HDAC1 and 2 mRNA in 3T3-L1 CAR adipocytes. *D–F*: Effect of HDAC1/2 knockdown on the expression of *TNF*, *IL6*, *MCP1*, *MCP2*, *MCP3*, and *Chop* genes (*D*), lipolysis (*E*), and JNK activation (*F*). *G*: Coimmunoprecipitation of SNRK, EEF1D, and HDAC1 from the overexpression study. *H*: HDAC1 activity in gonadal WAT of $SNRK^{fat-/-,\ A\text{-}Cre}$ and littermate control mice (n = 3 or 4 mice/group). IP, immunoprecipitation; TSA, trichostatin A (a pan HDAC inhibitor); WB, Western blot. *$P < 0.05$, shGFP vs. shEEF1D or shGFP vs. shHDAC1+2.

fed a chow diet, whereas homozygous loss of SNRK in adipocytes caused body weight to increase. This discrepancy may be attributed to as yet unknown functions of SNRK in nonadipose tissue. In our study, the increased body weight caused by adipose tissue–specific SNRK knockout can be explained by decreased energy expenditure. Furthermore, $SNRK^{fat-/-,\ A\text{-}Cre}$ mice are fully resistant to β3 adrenergic receptor agonist (CL316,243)–induced body weight reduction

and have a lower core body temperature in response to exposure to cold, which demonstrates that impaired thermogenesis likely causes the decreased energy expenditure in adipose tissue–specific knockout mice.

BAT is a key site of thermogenesis in mammals and for many decades has been considered to be an attractive target to control body weight. Brown adipocytes in BAT are packed with mitochondria containing UCP1. The activated UCP1 short-circuits the electrochemical gradient, oxidizes substrate quickly (with a low rate of ATP production), and generates heat (42). Thermogenesis in mature brown adipocytes is activated by norepinephrine, which is released from sympathetic neurons. Norepinephrine signals through β-adrenoreceptors to increase the expression and activity of PGC-1α, which is recognized as a master regulator of mitochondrial biogenesis and oxidative metabolism and induces the transcription of downstream thermogenic genes, including *UCP1* (43,44). Mechanistic studies further suggest that PGC-1α physically interacts with PRDM16 zinc-finger domains (45) and also coactivates peroxisome proliferator–activated receptor γ (46), C/EBPβ (47), and ZFP516 (48) via direct binding and then promotes expression of brown fat–selective genes. In our study, SNRK deletion in adipocytes disrupted mitochondria morphology and decreased mitochondria density. Furthermore, homozygous loss of SNRK in adipocytes resulted in a blunted response to CL316,243-induced UCP1, PRDM16, and PGC-1α expression in BAT. Based on these results , SNRK may play a key regulatory role in BAT thermogenesis upstream from these well-known thermogenic pathways.

To better extrapolate our findings from animal models to humans, we also analyzed human genetics to provide additional support for SNRK as an important regulator of adipose energy homeostasis. However, a few limitations should be kept in mind when interpreting the findings of our human study. First, although the two single nucleotide polymorphisms locate near several transcription factor binding sites and enhancer/promoter regions, their exact functions remain unknown. Second, we mainly focused on the common variants (minor allele frequency $\geq$0.05), whereas rare variants manifest a larger effect (49); other types of genetic variants, such as copy-number variations, were not considered in this study. Third, future work is needed to identify the precise genetic effects of SNRK and the relevant causal molecular variant(s) in men.

In summary, using both molecular experiments in knockout mice and genetic analysis of a human cohort, we provide strong evidence to show that SNRK represses WAT inflammation and is an essential factor in maintaining BAT thermogenesis. Enhancing SNRK function could have dual benefits on attenuating WAT inflammation and increasing BAT energy expenditure, which makes SNRK a novel potential therapeutic target for treating obesity and its complications.

Funding. Support for this work was provided by the National Institute of Diabetes and Digestive and Kidney Diseases (R01 DK103699 to H.X.). S.L. was supported by the American Heart Association (HHSN268201100003 and the Ahar Branch, Islamic Azad University [CVDGPS pathways grant]) and by the National Science Foundation (NSF 1557467 QuBBD). This work was also supported by the National Institutes of Health (NIGMS 8P30 GM103410, awarded to the transgenic core facility of Brown University). B.F. and P.J. are recipients of George A. Bray Research Scholars Awards from Brown University.

Duality of Interest. No potential conflicts of interest relevant to this article were reported.

Author Contributions. J.L. and B.F. developed the animal model and performed phenotyping. J.L., X.L., M.H., and S.L. performed the human genetics study. J.L., S.L., and H.X. wrote the manuscript. Y.N. and P.J. regulated the *SNRK* gene regulation and screened for embryonic stem cells. R.A., Q.H., and H.E.Z. assisted with the animal studies. A.S. performed the phosphoproteomic study. K.S.S. injected embryonic stem cells and bred the F1 generation for germline transmission. Z.W. studied oxygen consumption by primary brown adipocytes. S.L. supervised the human genetics study and provided logistical and administrative support. H.X. conceived the idea and supervised all animal studies. H.X. and S.L. are the guarantors of this work and, as such, had full access to all the data in the study and take responsibility for the integrity of the data and the accuracy of the data analysis.

References

1. Hotamisligil GS. Inflammation, metaflammation and immunometabolic disorders. Nature 2017;542:177–185
2. Xu H, Barnes GT, Yang Q, et al. Chronic inflammation in fat plays a crucial role in the development of obesity-related insulin resistance. J Clin Invest 2003;112:1821–1830
3. Liu J, Divoux A, Sun J, et al. Genetic deficiency and pharmacological stabilization of mast cells reduce diet-induced obesity and diabetes in mice. Nat Med 2009;15:940–945
4. Nishimura S, Manabe I, Nagasaki M, et al. CD8+ effector T cells contribute to macrophage recruitment and adipose tissue inflammation in obesity. Nat Med 2009;15:914–920
5. Winer S, Chan Y, Paltser G, et al. Normalization of obesity-associated insulin resistance through immunotherapy. Nat Med 2009;15:921–929
6. Feuerer M, Herrero L, Cipolletta D, et al. Lean, but not obese, fat is enriched for a unique population of regulatory T cells that affect metabolic parameters. Nat Med 2009;15:930–939
7. Weisberg SP, McCann D, Desai M, Rosenbaum M, Leibel RL, Ferrante AW Jr. Obesity is associated with macrophage accumulation in adipose tissue. J Clin Invest 2003;112:1796–1808
8. Osborn O, Olefsky JM. The cellular and signaling networks linking the immune system and metabolism in disease. Nat Med 2012;18:363–374
9. Aouadi M, Tencerova M, Vangala P, et al. Gene silencing in adipose tissue macrophages regulates whole-body metabolism in obese mice. Proc Natl Acad Sci U S A 2013;110:8278–8283
10. Clément K, Viguerie N, Poitou C, et al. Weight loss regulates inflammation-related genes in white adipose tissue of obese subjects. FASEB J 2004;18:1657–1669
11. Cancello R, Henegar C, Viguerie N, et al. Reduction of macrophage infiltration and chemoattractant gene expression changes in white adipose tissue of morbidly obese subjects after surgery-induced weight loss. Diabetes 2005;54:2277–2286
12. Kothari V, Galdo JA, Mathews ST. Hypoglycemic agents and potential anti-inflammatory activity. J Inflamm Res 2016;9:27–38
13. Scheen AJ, Esser N, Paquot N. Antidiabetic agents: potential anti-inflammatory activity beyond glucose control. Diabetes Metab 2015;41:183–194
14. Lancaster GI, Febbraio MA. The immunomodulating role of exercise in metabolic disease. Trends Immunol 2014;35:262–269
15. Feng B, Zhang T, Xu H. Human adipose dynamics and metabolic health. Ann N Y Acad Sci 2013;1281:160–177
16. Harms M, Seale P. Brown and beige fat: development, function and therapeutic potential. Nat Med 2013;19:1252–1263
17. Li Y, Nie Y, Helou Y, et al. Identification of sucrose non-fermenting-related kinase (SNRK) as a suppressor of adipocyte inflammation. Diabetes 2013;62:2396–2409

18. Koh HJ, Toyoda T, Fujii N, et al. Sucrose nonfermenting AMPK-related kinase (SNARK) mediates contraction-stimulated glucose transport in mouse skeletal muscle. Proc Natl Acad Sci U S A 2010;107:15541–15546
19. Rune A, Osler ME, Fritz T, Zierath JR. Regulation of skeletal muscle sucrose, non-fermenting 1/AMP-activated protein kinase-related kinase (SNARK) by metabolic stress and diabetes. Diabetologia 2009;52:2182–2189
20. Ichinoseki-Sekine N, Naito H, Tsuchihara K, et al. Provision of a voluntary exercise environment enhances running activity and prevents obesity in Snark-deficient mice. Am J Physiol Endocrinol Metab 2009;296:E1013–E1021
21. Yoshida K, Yamada M, Nishio C, Konishi A, Hatanaka H. SNRK, a member of the SNF1 family, is related to low K(+)-induced apoptosis of cultured rat cerebellar granule neurons. Brain Res 2000;873:274–282
22. Rines AK, Burke MA, Fernandez RP, Volpert OV, Ardehali H. Snf1-related kinase inhibits colon cancer cell proliferation through calcyclin-binding protein-dependent reduction of β-catenin. FASEB J 2012;26:4685–4695
23. Chun CZ, Kaur S, Samant GV, et al. Snrk-1 is involved in multiple steps of angioblast development and acts via notch signaling pathway in artery-vein specification in vertebrates. Blood 2009;113:1192–1199
24. Pramanik K, Chun CZ, Garnaas MK, et al. Dusp-5 and Snrk-1 coordinately function during vascular development and disease. Blood 2009;113:1184–1191
25. Cossette SM, Gastonguay AJ, Bao X, et al. Sucrose non-fermenting related kinase enzyme is essential for cardiac metabolism. Biol Open 2014;4:48–61
26. Rines AK, Chang HC, Wu R, et al. Snf1-related kinase improves cardiac mitochondrial efficiency and decreases mitochondrial uncoupling [published correction appears in Nat Commun 2017;8:16155]. Nat Commun 2017;8:14095
27. Cossette SM, Bhute VJ, Bao X, et al. Sucrose nonfermenting-related kinase enzyme-mediated rho-associated kinase signaling is responsible for cardiac function. Circ Cardiovasc Genet 2016;9:474–486
28. Klein J, Fasshauer M, Klein HH, Benito M, Kahn CR. Novel adipocyte lines from brown fat: a model system for the study of differentiation, energy metabolism, and insulin action. BioEssays 2002;24:382–388
29. Orlicky DJ, DeGregori J, Schaack J. Construction of stable coxsackievirus and adenovirus receptor-expressing 3T3-L1 cells. J Lipid Res 2001;42:910–915
30. Jiao P, Chen Q, Shah S, et al. Obesity-related upregulation of monocyte chemotactic factors in adipocytes: involvement of nuclear factor-kappaB and c-Jun NH2-terminal kinase pathways. Diabetes 2009;58:104–115
31. Jaleel M, McBride A, Lizcano JM, et al. Identification of the sucrose non-fermenting related kinase SNRK, as a novel LKB1 substrate. FEBS Lett 2005;579:1417–1423
32. Montgomery RL, Davis CA, Potthoff MJ, et al. Histone deacetylases 1 and 2 redundantly regulate cardiac morphogenesis, growth, and contractility. Genes Dev 2007;21:1790–1802
33. Montgomery RL, Hsieh J, Barbosa AC, Richardson JA, Olson EN. Histone deacetylases 1 and 2 control the progression of neural precursors to neurons during brain development. Proc Natl Acad Sci U S A 2009;106:7876–7881
34. Yamaguchi T, Cubizolles F, Zhang Y, et al. Histone deacetylases 1 and 2 act in concert to promote the G1-to-S progression. Genes Dev 2010;24:455–469
35. LeBoeuf M, Terrell A, Trivedi S, et al. Hdac1 and Hdac2 act redundantly to control p63 and p53 functions in epidermal progenitor cells. Dev Cell 2010;19:807–818
36. Feng B, Jiao P, Helou Y, et al. Mitogen-activated protein kinase phosphatase 3 (MKP-3)-deficient mice are resistant to diet-induced obesity. Diabetes 2014;63:2924–2934
37. Kawaguchi Y, Kato K, Tanaka M, Kanamori M, Nishiyama Y, Yamanashi Y. Conserved protein kinases encoded by herpesviruses and cellular protein kinase cdc2 target the same phosphorylation site in eukaryotic elongation factor 1delta. J Virol 2003;77:2359–2368
38. Chang YW, Traugh JA. Insulin stimulation of phosphorylation of elongation factor 1 (eEF-1) enhances elongation activity. Eur J Biochem 1998;251:201–207
39. Haberland M, Montgomery RL, Olson EN. The many roles of histone deacetylases in development and physiology: implications for disease and therapy. Nat Rev Genet 2009;10:32–42
40. Grausenburger R, Bilic I, Boucheron N, et al. Conditional deletion of histone deacetylase 1 in T cells leads to enhanced airway inflammation and increased Th2 cytokine production. J Immunol 2010;185:3489–3497
41. Turgeon N, Blais M, Gagné JM, et al. HDAC1 and HDAC2 restrain the intestinal inflammatory response by regulating intestinal epithelial cell differentiation. PLoS One 2013;8:e73785
42. Ricquier D. Uncoupling protein 1 of brown adipocytes, the only uncoupler: a historical perspective. Front Endocrinol (Lausanne) 2011;2:85
43. Tiraby C, Tavernier G, Lefort C, et al. Acquirement of brown fat cell features by human white adipocytes. J Biol Chem 2003;278:33370–33376
44. Puigserver P, Wu Z, Park CW, Graves R, Wright M, Spiegelman BM. A cold-inducible coactivator of nuclear receptors linked to adaptive thermogenesis. Cell 1998;92:829–839
45. Seale P, Kajimura S, Yang W, et al. Transcriptional control of brown fat determination by PRDM16. Cell Metab 2007;6:38–54
46. Seale P, Bjork B, Yang W, et al. PRDM16 controls a brown fat/skeletal muscle switch. Nature 2008;454:961–967
47. Kajimura S, Seale P, Kubota K, et al. Initiation of myoblast to brown fat switch by a PRDM16-C/EBP-beta transcriptional complex. Nature 2009;460:1154–1158
48. Dempersmier J, Sambeat A, Gulyaeva O, et al. Cold-inducible Zfp516 activates UCP1 transcription to promote browning of white fat and development of brown fat. Mol Cell 2015;57:235–246
49. Gibson G. Rare and common variants: twenty arguments. Nat Rev Genet 2012;13:135–145